CHAPTER 1

INTRODUCTION AND LITERATURE REVIEW

1.1 Noble Metal Nanoparticles

Development of stable colloidal suspension of nanoparticles has opened up new vistas of activities in the diverse fields of science and engineering. It has been made possible owing to availabilities of control synthesis of nanostructured materials. The unique properties that result from these materials have been utilized to solve problems in a plethora of disciplines ranging from solar energy conversion and catalysis to biomedicine and agriculture [1–4]. Noble metal nanoparticles (NPs) are of particular interest for many of the applications. The distinct physical and chemical properties that these materials possess have made them important class of materials for applications. When the dimensions of noble metal particles are reduced into the nanometer regime, the materials can exhibit properties that are different from their bulk counterparts owing to effects such as quantum confinement and increased surface area [5]. For example, decreasing the size of the particles into the nanoscale enhances the exposed surface area of the material leading to increased chemical reactivity. This phenomenon has been especially useful in catalysis. The NPs of platinum and palladium has displayed a dramatic improvement in catalytic activity compared to their bulk counterparts [6, 7]. Changes in shapes of noble metal NPs can also have a pre-dominant impact on the catalytic and chemical reactivity of the nanoparticle surface [8]. Maneuvering preferential generation of specific crystal planes

through anisotropic particle formation, it is possible to improve the reactivity of the material. It has been demonstrated that platinum nanowires, for example, have higher catalytic activity than platinum spheres because of the exposure of the (110) crystal planes [9].

Optical properties emerging out of collective oscillation of the surface electrons in noble metal NPs are also of interest for plasmonic applications (cf. section 1.9). This collective oscillation is often referred to as a localized surface plasmon resonance (LSPR) and results in a characteristic absorbance band, typically in the ultraviolet and visible region of the electromagnetic spectrum [10]. The LSPR behavior of metal NPs makes them suitable for a range of applications in areas like miniaturized optical devices, photonic circuitry, biological imaging, and optically targeted drug delivery [11–14]. Altering the size and shapes of these nanomaterials, it is possible to vary the frequency at which the surface electrons oscillate [15]. The LSPR has been studied extensively in NPs of Au and Ag where variety of shapes and sizes are easily accessible [16, 17]. The nanoshells of Au can be synthesized with a variable shell thickness [18]. The resulting LSPR band of the nanoshells can then be red shifted by either increasing the shell diameter, or decreasing the shell thickness.

As the applications of these materials begin to require more sophisticated control of the nanomaterial properties, the synthetic techniques employed in the generation of these materials will require more precise control over the resulting size, composition, and morphology. Synthesis of copper nanoparticles (Cu NPs) is important due to their optical, electrical and thermal properties [19]. Synthesis of Cu NPs is cost effective when compared to silver (Ag), gold (Au) and platinum (Pt) [20]. Synthesis of stable Cu NPs is a

challenging task and various methods have been developed to synthesize Cu NPs including physical, chemical and biological processes [21]. A precise control of the shape and size of these NPs is essential for the applications in the optics, electronics, and catalysis. Apart from this, the NPs needed to be compatible with biological systems for their applications in biology and medicine [22–24]. Therefore, green processes are being sought after.

The methods used to synthesize these materials can in general, be classified as "top-down" or "bottom-up" approaches. In top-down approaches, a bulk material is reduced to the nanoscale through a high energy process. Examples of such a process include ball-milling, laser ablation, etc. [25, 26]. These methods normally involve complex experimental setups, harsh reaction conditions, and in general, do not provide much control in the final material yield and morphology at submicroscopic level. In the alternative bottom-up approaches, NPs are generated by nucleation from atomic or molecular precursors and subsequently grown into the desired morphologies of NPs. Examples of such techniques include flame spray synthesis, chemical vapor deposition, the sol-gel process, and other solution based methods [27, 28]. These approaches typically result in a high degree of control over particle morphology and composition due to the relatively low temperatures and the ability to precisely tune the particle growth through precursor concentration, reducing agents, molecular and polymeric surface stabilizers, pH (aqueous solution) and other reagents. These chemicals allow for surface modification which can result in colloidal stability. Wet chemical methods also enable the use of surface stabilizers which can facilitate more control over the growth direction and surface chemistry

of the resulting NPs [15]. Wet chemical synthesis of NPs has been shown to be sensitive to small variation in reagent concentration, often resulting in dramatic change in particle morphology. For example, it has been reported that minute changes in halide concentration can give rise to different morphology such as spheres, rods, and plates in aqueous Au nanoparticle synthesis [29]. This sensitivity coupled with the limited volumes of reaction chamber, makes large scale production of these materials difficult by wet chemical methods. Despite these limitations, wet chemical methods have provided a diverse library of tunable sizes and shapes for a variety of materials. These methods have also been shown to generate complex nanostructures, such as core-shell NPs where one inorganic material completely encapsulates another [30–32]. These advanced materials provide a wider range of functionalities for noble metal NPs by incorporating the functionality of multiple inorganic substances containing various compositions and morphologies within the same nanoscale material.

1.2 Oriented Attachment

As mentioned earlier, wet chemical syntheses have been extensively studied and employed to fabricate solid nanocrystals with well-defined sizes and shapes. Studies of the growth of these nanocrystals are both interesting and beneficial. From a fundamental standpoint, many crystals in solution grow via Ostwald ripening [33], in which the larger nanocrystals grow atom-by-atom, at the expense of smaller ones. An alternate or parallel mechanism is cluster aggregation, which often leads to the formation of random and ill-formed agglomerates. However, cluster aggregation is not always random. As Penn and Banfield [34]

demonstrated, cluster aggregation can occur along specific crystallographic directions and lead to the formation of single (lattice matching attachment, MA) or twinned (twinned attachment, TA) crystals. This non-random aggregation is known as oriented attachment (OA). Driving force for OA is thought to be reduction in interfacial energy based on several reports in literature [35–41]. For example, in a recent experiment [41] with high resolution transmission electron microscopy (HRTEM) in a liquid cell have allowed for in situ imaging of OA. They observed that particles of iron oxide undergo continuous rotation and interaction until they find a perfect lattice match.

1.3 Ag, Au, and Cu nanoparticles

Gold NPs are one of the earliest examples of colloidally stable NPs and are widely used for their strong optical properties [42]. It is possible to generate colored glass for example, by adding finely processed gold to glass [43]. The vibrant red-wine colors that result were attributed first by Faraday to be the result of the small size of the particulate gold [44]. This color is the result of the surface plasmon resonance of the material and is subsequently dependent on the particle morphology. Spherical gold NPs, for example, can possess a plasmon band typically ranging from 520 nm to the infra-red regime depending on the particle size and shape. This optical activity, combined with the biocompatibility of gold, have allowed for these materials to be used in genetic manipulation, anti-cancer therapy, and medical imaging [45, 46]. The library of shapes that has been demonstrated thus far includes spheres, rods, plates, wires, ribbons, octahedral, and shells in addition to many others [47–50]. Many of the applications of these materials depend on the ability

to intelligently modify the optical properties. One method of altering the surface plasmon of gold NPs is to alter the morphology of these materials. For example, aqueous gold NPs can be synthesized with progressively increasing aspect ratios [51]. This results in a progressive red shift in the plasmon band, resulting in tunability from the visible into the infrared. The face centered cubic gold has been reported to form different phases depending on size and shape of gold crystallites. The phases refer to tetragonal, orthorhombic, and hexagonal [52, 53]. All these phases have distinct structural characteristics and depict different face forms apart from usual pentagonal twins observed in gold particles both in native and synthetic state [52, 53]. The optical properties of gold NPs have also been modified by alloying the particle with another metal. The resulting plasmon band behaves as a hybrid of the two materials, and possesses variability based upon the proportion incorporated. Au has been previously shown to form alloy NPs with other optically active metals such as Cu and Ag [54–58]. This ability to tune material properties via composition combined with the wide variety of shapes available makes gold NPs an important candidate for investigations both in elemental as well as in alloy form.

1.4 Alloy Nanoparticles

Many of the current applications of noble metal NPs depend on the ability to intelligently control the functional properties of the material. One method of exercising such control is through formation of alloys and intermetallic compounds. Alloys behave as a solid solution having varied range of solid solubilities or complete miscibility in the solid state. Intermetallic compounds posses different crystal structures than those of the

components unlike solid solution. They are formed in narrow range of compositional variations. They display order-disorder transformations. When these materials are incorporated into nanoparticle systems, synergistic effects in addition to property tunability can be observed. Alloy NPs comprised of nickel and palladium, for example, have been shown to synergistically enhance the catalysis of coupling reactions. The resulting catalytic activity of the alloy NPs was greater than the activity of the single metal nanoparticle. These materials are traditionally generated through intimately mixing the constituent atoms together in the form of bulk powders at high temperatures over long periods of time. This process is energy intensive but necessary to ensure uniform diffusion throughout the material. When NPs are used instead of bulk powders, the speed at which this formation occurs can be greatly increased. Since the diffusion distances are much shorter in nanoparticle systems, the formation of alloy NPs can proceed at much lower temperatures with much shorter reaction times[59]. This allows solution based synthesis of alloy NPs at relatively lower temperatures. Formation of non-equilibrium and metastable phases is often seen at nanoscale owing to defects. These phases are not thermodynamically favored under the conditions present in traditional solid-state methods but often become stable for kinetic reasons [60, 61]. Solution methods offer multiple approaches for the synthesis of alloy and intermetallic NPs. One approach involves first generating a nanoscale composite with the desired stoichiometry through either co-reduction of salt precursors or physical mixture of discrete NPs, and subsequently heating the composite until the desired phase is achieved [62]. An illustration of this process is shown in Figure 1.1. Although this method allows for excellent control over chemistry of the products, the amount of sintering that occurs

results in a lack of control over the particle size and shape. Another approach involves the use of pre-made NPs as a template for conversion chemistry. In this approach, stable suspensions of NPs are transformed into alloy or intermetallic compounds through chemical processes that can include diffusion, ion-exchange, or galvanic replacement [63–67]. An illustration of this process is shown in Figure 1.2. This method has been shown to be applicable to a variety of precursors and often maintains the morphology of the original template NPs. This has the benefit of allowing for modulation in chemistry without changing the size and shape of the material. An additional method involves the co-reduction of metal cations in solution to generate the desired nanoparticle. In this approach, two or more types of metal cations are thoroughly dissolved in solution and are simultaneously reduced via thermal or chemical means [68]. An illustration of this approach is shown in Figure 1.3. Presence of surfactants and other chemicals into this method can often result in nanoparticle monodispersity and shape control. Although the composition of the final product can be controlled by altering the precursor ratios, this method is sensitive to changes in the reduction rate. Thus, changes in the reducing agent and temperatures used during the synthesis will often result in different nanoparticle shapes and chemistry. These solutions based routes have been used to generate composition-tunable systems involving noble metal NPs. Alloy NPs containing gold and silver for example have been prepared in aqueous solution through a solution based co-reduction route [69]. The resulting optical properties of the material were found to vary linearly with the mole fraction of metal ions used. This composition based tuning of optical activity has also been demonstrated for a variety of silver and gold nanoparticle based systems including silver-copper and

gold-copper, making silver and gold containing alloy and intermetallic NPs an attractive target for composition control studies and applications. The Ag-Cu and Au-Cu alloys at nanoscale have been synthesized and studied in detail. Such studies shall form major part of this investigation. Literature related to syntheses and LSPR activities of these alloys is presented in subsequent sections.

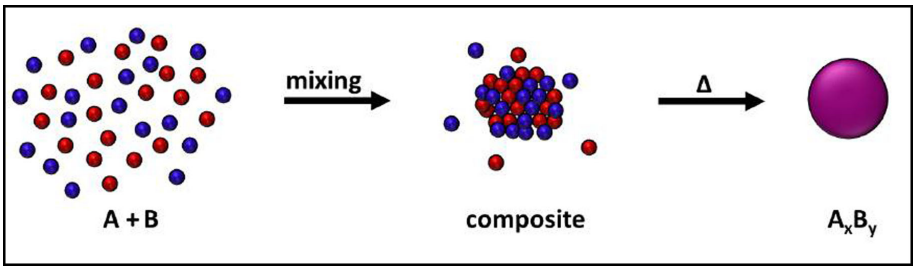

FIGURE 1.1: Illustration of synthesis of bimetallic NPs of desired stoichiometry where A and B represents metal I and metal II, respectively.

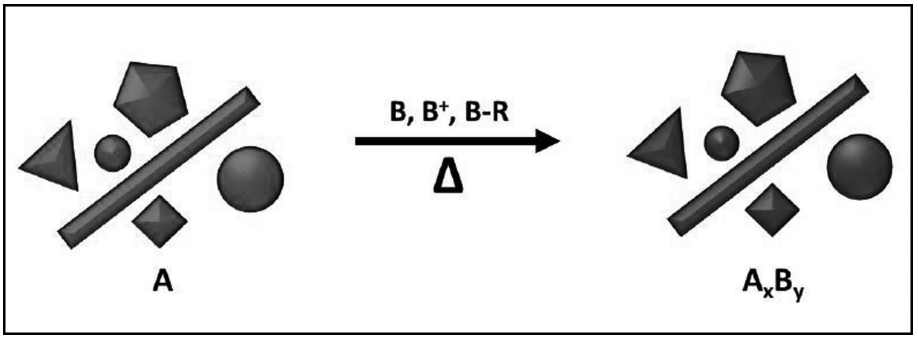

FIGURE 1.2: Depiction of shape controlled synthesis of bimetallic NPs of desired stoichiometry where A represents metal I. The B, B^+ and B-R correspond to elemental, ionic and organometallic precursors of metal II, respectively.

1.5 Ag-Cu Alloy Nanoparticles

For the metallic salt reduction process, the metal species with the highest redox potential generally precipitates first, forming a core on which the second component is deposited

in the case of alloy nanoparticle [71, 72]. In this thesis, Ag-Cu alloy NPs have been synthesized with chemical reduction methods. This was achieved by using hydrazine hydrate and rice-starch as reducing agent and stabilizers respectively. Rice-starch serves as stabilizers making the synthesis process and the NPs more environmental friendly. The segregation of silver and copper metal during Ag-Cu nanoparticle formation is another area of investigation since heterogeneous spatial distribution of the metal elements caused by

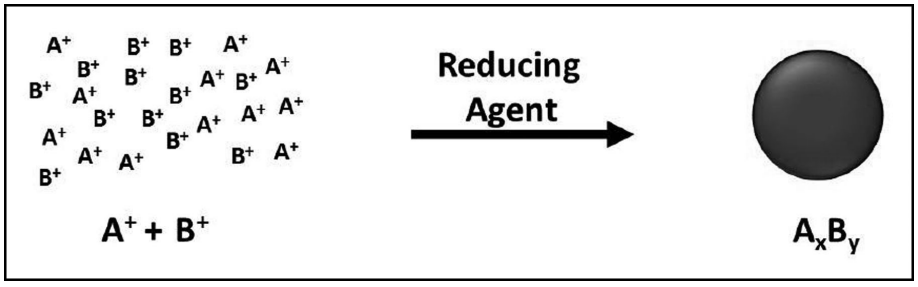

FIGURE 1.3: Schematic displaying coreduction strategy to synthesize bimetallic NPs. Metals precursor A^+ and B^+ are in cationic form.

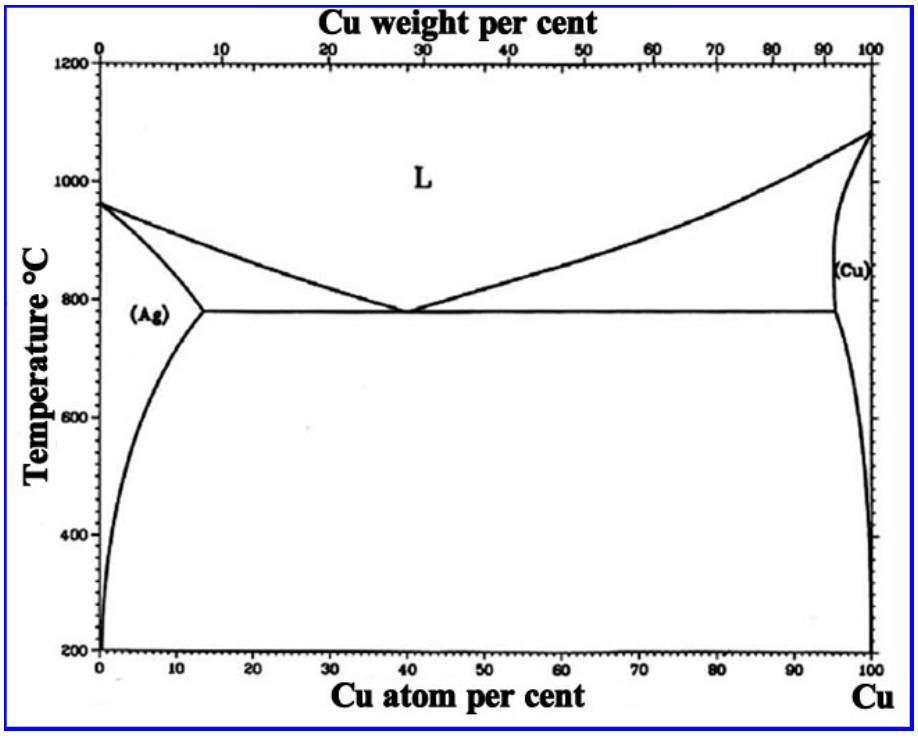

FIGURE 1.4: Equilibrium phase diagram of Ag-Cu system [70].

surface segregation, for example, could influence the rate at which the metals in the alloy NPs are oxidized and released into solution. Since Cu NPs could be used, in several applications, as a substitute for very expensive noble metals such as silver, recent years have seen interest in Ag-Cu core-shell particles [73–75]. Consideration of the Ag-Cu phase diagram shows that one expects a phase field consisting of Ag and Cu owing to extremely low solid solubilities below 200 ºC (Figure 1.4) [70]. With a positive solid phase mixing enthalpy ($\Delta H_{mix} > 0$), Ag and Cu atoms tend to separate, and the most stable state is a mixture of two phases. Ag core- Cu shell clusters have been generated experimentally by radiolysis of solutions containing copper and silver sulfate [76]. Recently, other research groups have applied chemical reduction methods to synthesize Ag/Cu [73–75, 77–79]. Their results did not give very strong evidence of core-shell structures in Ag-Cu NPs. On the contrary, Jiang et al. found both silver and copper (111) lattice planes in a particle as one would expect from the phase diagram [78]. Grouchko et al. have shown the formation of highly stable Cu core- Ag shell in a two step chemical method [79]. They prepared Cu NPs in the first step followed by addition of $AgNO_3$ in varying amounts. The synthesis scheme is illustrated in Figure 1.5.

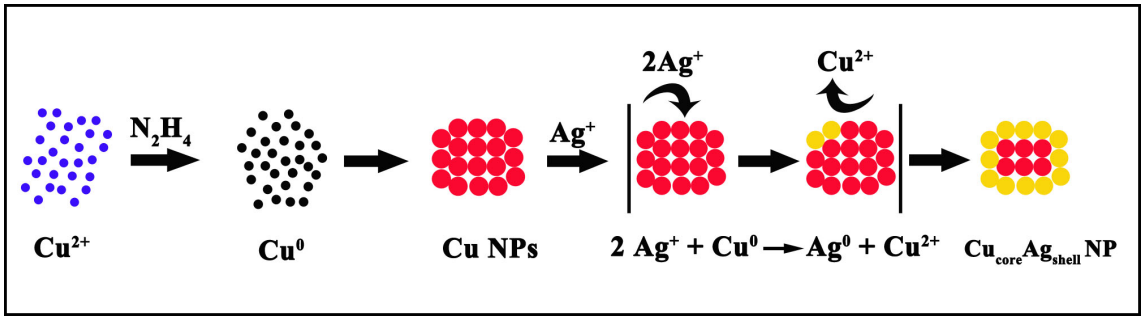

FIGURE 1.5: Illustration of Cu core-Ag shell NPs synthesis adopted from Grouchko et al. [79].

1.6 Au-Cu Alloy Nanoparticles

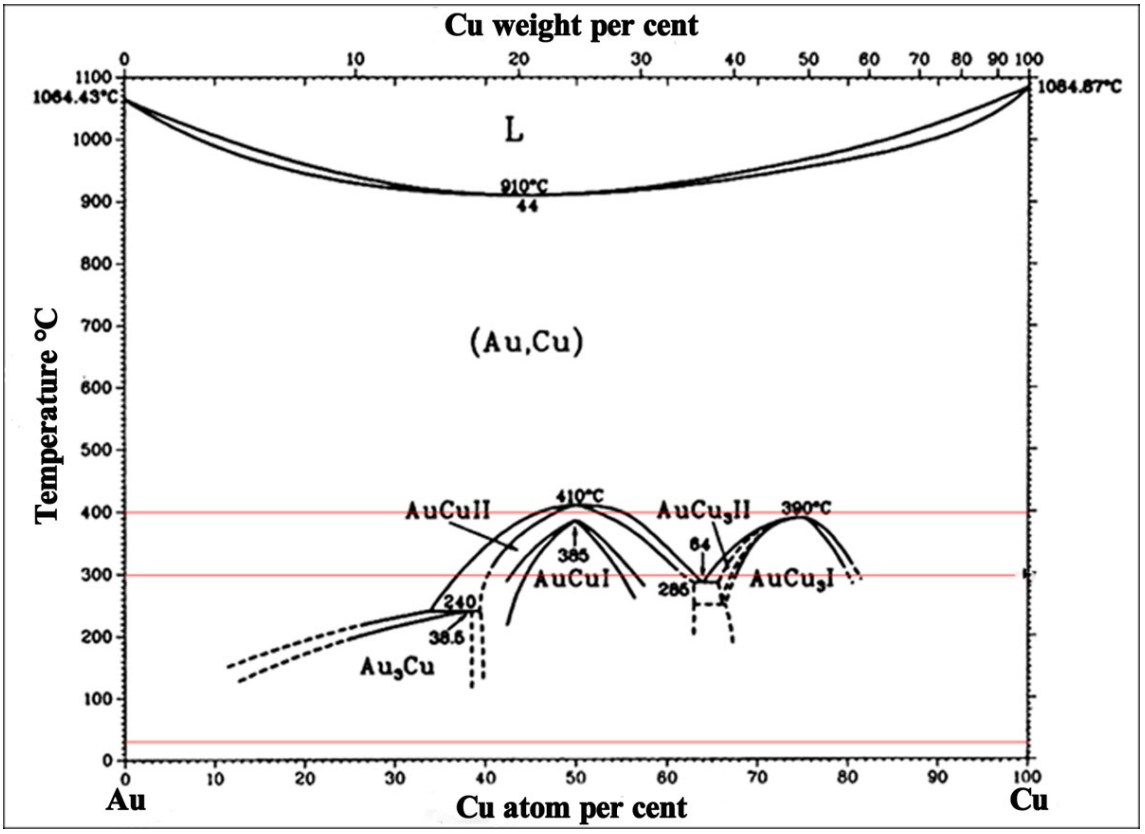

FIGURE 1.6: Equilibrium phase diagram of Au-Cu system [80] .

According to empirical Hume–Rothery rules, whether an alloy can be formed with two metals depend on the similarity of four factors: atomic radii, valence, crystal structure and electronegativity [81, 82]. The elements Au and Cu satisfy three of these conditions as they share common crystal structure (FCC), valence (+1) and similar atomic radii (difference less than 15%). As a consequence of this, one notes single phase field solid solution forming for the entire compositional range between $\sim$ 410 ºC to $\sim$ 910 ºC. However, interesting features are observed in the compositional range of $\sim$ 10 at.% Cu to $\sim$ 81 at.% below 400 ºC. They refers to formation of $AuCu_3$, Au_3Cu and AuCu intermetallic compounds as well as order-disorder transformation (Figure 1.6) [80]. The

composition alone is not sufficient to describe alloy NPs as their properties are correlated to the nature of atomic ordering (i.e., random alloy versus intermetallic compound) even when they are exactly identical in terms of composition and stoichiometry [83–85]. This difference can arise owing to the changes in crystal structure and surface structure. These features can modulate the strength and nature of how chemical species adsorb and react, respectively, leading to different functional properties [86–89]. It has been established by a large number of studies that conversion from alloy NPs by heat treatment in an inert medium is the most effective method for the formation of intermetallic NPs, irrespective of strategy used to synthesize alloy NPs [90, 91]. However, heat treatments may lead to aggregation and Ostwald ripening in the NPs giving rise to bigger particles and broader size distributions [92]. In addition to size and uniformity, there are strong efforts to develop shape-controlled syntheses of intermetallic NPs. To avoid such limitations, seed-based method has been demonstrated for the synthesis of intermetallic NPs, but in the solution phase [93]. This protocol generally involves two sub-steps: i) synthesis of seeds in the form of metal NPs, and ii) diffusion of atoms from the newly generated species including atoms, clusters, and small particles into the as-formed seeds. This synthesis method was initiated by Cable and Schaak [93], and they reported the growth of intermetallic M–Zn nanocrystals (M = Au, Cu, and Pd) through seed-based growth utilizing organoamine solvents. Such a synthesis leads to modification in size, shape, as well as internal structure of the product phase. This has been shown by Li and co-workers in the synthesis of uniform 5-fold twinned AuCu intermetallic nanocrystals with a size of $\sim$ 10 nm by employing pseudo-icosahedral or decahedral Au nanocrystals as seeds in a

mixture of oleic acid and tri-n-octylamine at 280 °C [94]. In this synthesis, the newly reduced Cu atoms or clusters with high reactivity rapidly diffused into the 5-fold twinned Au seeds as driven by the thermal energy, leading to the formation of $L1_0$ AuCu intermetallic nanocrystals (tetragonal). By increasing the amount of the Cu precursor, the $L1_2$ $AuCu_3$ (cubic) intermetallic nanocrystals were generated at a higher reaction temperature of 300 °C. Due to the strong interaction of oleic acid with intermetallic nanocrystals, anisotropic growth was restricted in this system. In another investigation, Ying et al. demonstrated the anisotropic growth of intermetallic AuCu pentagonal nanorods by replacing a mixture of oleic acid and tri-n-octylaminewith oleylamine [95]. Intermetallic AuCu pentagonal nanorods were preferentially grown from the multiply twinned decahedral Au seeds along their $< 110 >$ directions due to the preferential adsorption of oleylamine on the $\{100\}$ facets. Utilizing this scheme, structure and composition of the intermetallic AuCu pentagonal nanorods could be easily manipulated by varying the number of Au seeds and their molar ratio relative to the Cu precursor, respectively. In another study, Jin and coworkers reported the synthesis of Au_3Cu intermetallic truncated nanocubes with sizes of 15–30 nm through the chemical conversion of Cu microparticles in a mixture containing oleylamine, trioctylphosphine (TOP), and $AuPPh_3Cl$ at 200 °C [96]. The synthesis was initiated by a galvanic replacement reaction occurring between the Cu microparticles and the Au precursor, leading to the formation of single crystalline Au nanocrystals and Cu^{2+} ions. Afterward, the newly formed Cu^{2+} ions were reduced to Cu atoms by oleylamine, followed by diffusion into the single-crystal Au seeds to produce intermetallic truncated nanocubes. Interestingly, only Au_3Cu intermetallics could be synthesized, even when

the Cu precursor was in excess, because this phase is the most thermodynamically stable among three types of Au–Cu intermetallic compounds (i.e., Au_3Cu, AuCu, and $AuCu_3$) [96].

1.7 Order-disorder transformation

Bimetallic NPs prepared through wet-chemical syntheses typically take a random, alloy structure and are thus more prevalent than the intermetallic variants, even when the latter is favored thermodynamically at lower temperature. This outcome can be attributed to the relatively low temperatures intrinsic to most wet-chemical syntheses compared to the high activation energy barrier to inter-diffusion and thus equilibration. The total surface free energy increases as the size of a nanoparticle approaches down to a few nanometers, resulting in the rapid drop in the disorder-to-order transition temperature [97]. This effect has been repeatedly confirmed in various bimetallic systems such as Pt-Co, Pt-Fe, and Au-Cu with the assistance of *in situ* heating inside a transmission electron microscope [98–102]. For example, Yasuda and co workers [102] investigated the mixing of Cu atoms in Au clusters with *in situ* TEM. At room temperature, they observed spontaneous mixing forming a solid solution and the diffusion coefficient of Cu was 9 orders of magnitude larger than that for Cu dissolution in bulk Au. At lower temperature, the mixing leads to a Au core surrounded by Cu-Au solid solution. The solid solution was also found at temperatures below the bulk order-disorder transition temperature. Experimental conditions may favor the intermetallic structure, complete transformation is typically never guaranteed within reasonable time frames due to the relatively high diffusion barriers. Different

from thermodynamics, the effect of size on the kinetics of the disorder-to-order transition is more complicated, generally including two opposite impacts. The increase in surface energy will reduce the driving force toward an ordered phase whereas surface diffusion can make a greater contribution to the atom transport in smaller NPs, with a much lower diffusion barrier to overcome relative to the bulk [103].

1.8 Role of vacancy in formation of new phases

The structural transformation in nanomaterials associated with vacancy and its ordering has not been dealt with previously in details. There are a few theoretical reports in literature related to structural modification of nanoparticles [104]. Gafner and Baidyshev [104] for example, demonstrated the effect of size and heat treatment on internal structural changes in Al clusters using molecular dynamics (MD) simulations. They reported that aluminum clusters with sizes up to 2.5 nm, the most stable configuration is the structure with pentagonal symmetry and with a further increase in the number of atoms, the FCC structure becomes more stable. They further showed that for clusters with diameter of 3 nm, an increase in the number of vacancies led to an increase in the number of clusters with icosahedrally related ones, whereas for clusters with the diameter 4 nm, the decahedral structure remains predominant. Such coordination polyhedra may give rise to structural transformations at nanoscale.

1.9 Optical properties of noble metal NPs

This section introduces the concepts required to understand the optical properties of noble metal nanoparticle sols. One of the methods to study optical properties is localized surface plasmon resonance (LSPR) behaviour of NPs has been described in subsequent sections.

1.9.1 Surface Plasmon Resonance

The physical origin of the strong light absorption by metal NPs is the collective oscillation of the conduction electrons induced by electromagnetic radiation. Such collective oscillation of conduction electrons in metals is known as plasmon. The formation and origin of plasmon in metals can be explained as follow. Metals can be considered as collection of positive ion cores and conduction electrons (confined plasma). Initially, charged clouds of electrons and ion cores overlap with each other. The electromagnetic radiation disturbs the charged cloud and electrons are moved away from the equilibrium position. If the density of electrons in one region increases, they tend to return to the equilibrium position due to repulsion between the electrons. This repulsion makes the electrons to move towards their equilibrium position with certain kinetic energy. Thus, they oscillate back and forth. As the net charge difference occurs at the nanoparticle's surface, the electrons on the surface are the most significantly involved in oscillations and their collective oscillations are known as surface plasmon. The resonance between these oscillations and incidence light gives rise to an intense peak in the visible range of the electromagnetic region and is known as surface plasmon resonance [105, 106]. The scattering of light by small particles

is explained with the help of Mie theory [107]. Figure 1.7 shows the displacement of conduction electron charge cloud relative to the nuclei of spherical nanoparticle and nanorod [108].

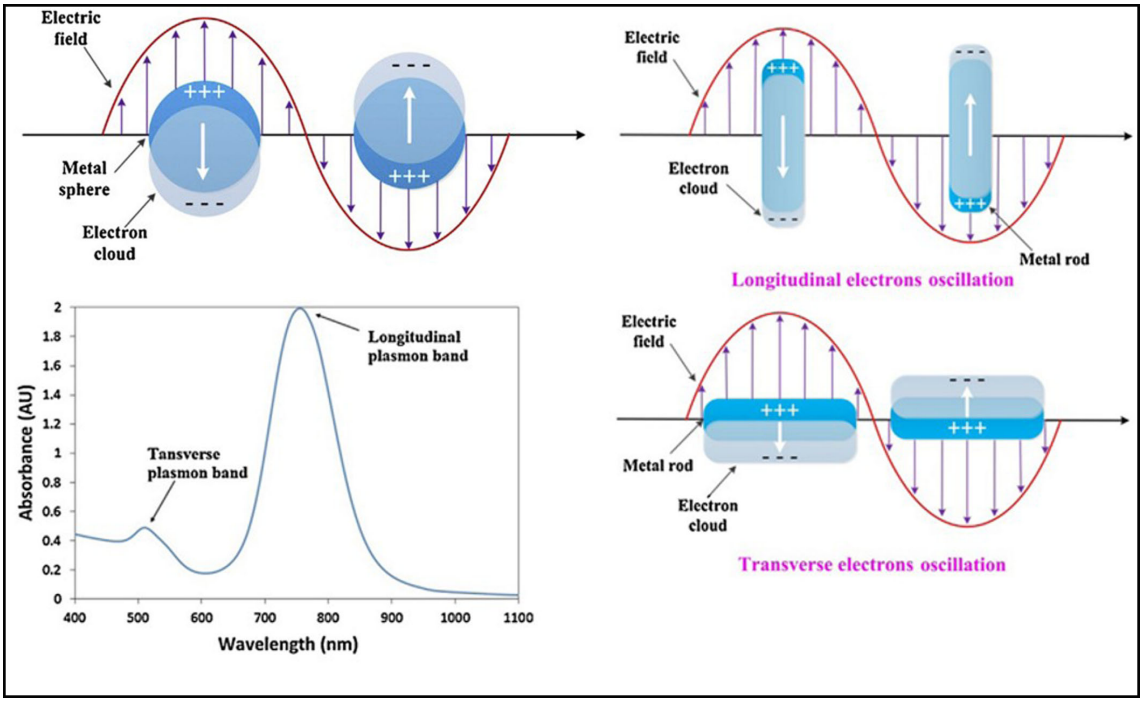

FIGURE 1.7: Plasmon oscillations for a sphere showing the displacement of conduction electron charge cloud relative to the nuclei. The transverse and longitudinal modes of oscillations from a nanorod and corresponding spectral manifestation as observed in UV-Vis absorbance spectrum [108].

1.9.2 Tuning the surface plasmon resonance band of metallic nanostructures

Silver and gold NPs have been studied for their unique optical properties in a wide spectral range of the particles and shapes. These particles show SPR band in the visible range of electromagnetic spectrum. The nature of spectra depends on various factors such as size, shape and dielectric constant of the medium in which they are dispersed [109–115]. These

SPR bands of metal NPs can be varied by changing their sizes in the range of 1 – 100 nm. In contrast, SPR band can be modulated from visible to near infrared region by varying the shape of the NPs [116]. The position of the SPR bands varied in the visible region with various morphologies and structures of Au and AgNPs. When a transition in shape from sphere to rod is made then a single plasmon absorption band splits into two as shown in Figure 1.7. At the higher wavelengths, a peak is observed due to longitudinal plasmon resonance (LSPR) along longer axis while at shorter wavelengths, a peak is observed due to transverse plasmon resonance (TSPR) along shorter axis [116].

1.9.3 Localized surface plasmon resonance (LSPR)

When size of the NPs is very small than the wavelength of incident radiation, the collective oscillation of free electrons is confined to a finite volume as in case of metal NPs. This phenomenon is called a localized surface plasmon resonance (LSPR). The LSPR can create intense electric field very close to (within a few nanometers) a particle surface resonance. This near field effect can improve Raman scattering cross sections for the molecules adsorbed onto the surface. Thus, the LSPR depends upon the surrounding medium refractive index of metal (Au, Ag, Al and Cu) NPs which are examined by the electrodynamics approach. However, the localization studies have been focused on Au and Ag NPs for many years because of their bulk dielectric properties [113, 117].

1.9.4 Effect of shape and size on LSPR

The frequency and intensity of plasmon resonance are determined by the intrinsic dielectric properties of the metals, dielectric constant of the medium which it is in contact with and surface polarization. Variation in shape and size of metallic NPs alters the spectral signature of its plasmon resonance. The ability to change shape and size of the particles and the study of its effect on LSPR is an important and challenging task. The interaction of an electromagnetic wave with NPs can be understood by Maxwell's equations [118]. Maxwell's equations, based on analytical formulations such as the Mie theory, are desirable for special cases such as solid sphere, concentric spherical shell, infinite cylinder, etc. [119]. Numerical calculations with some approximation are required for other particles having arbitrary geometrical shapes. Apart from above mentioned numerical approaches, the discrete dipole approximation (DDA) has also been used to simulate the interaction of light with metallic NPs with arbitrary shapes [120]. The discrete dipole interaction is used to investigate the effect of shape on LSPR. Dipole approximation calculations are integrated with experimental studies to achieve better understanding of LSPR spectra obtained from NPs sample [121]. These calculations also provide useful guidelines for the design and fabrication of novel plasmonic NPs [121]. Surface polarization is the most important factor in determining the frequency and intensity of plasmon resonance for a given metal nanoparticle because it provides the main restoring force for electron oscillation. Indeed, any variation in particle shape, size and a medium will change the surface polarization [122]. For example, nanocubes have several distinct symmetries for dipole resonance as compared to only one for the sphere and hence nanocubes exhibits more

peaks than the sphere [122]. The tetrahedron shows the red shifted resonance of three platonic sides because it has the sharpest corners [122].

1.9.5 LSPR behavior of Ag-Cu and Au-Cu Alloy Nanoparticles

The LSPR behaviour of bimetallic NPs is expected to be different than that of elemental NPs owing to variation of composition and crystal structures along with shape, size, and distribution. It was demonstrated by several researchers that position of LSPR band of Ag-Cu alloy NPs observed between Ag and Cu NPs [72, 77, 78, 123]. Valodkar et al. for example showed that LSPR peaks appeared at $\sim$ 416 and $\sim$ 584 nm corresponding to Ag and Cu NPs, respectively [77]. The red shift of LSPR peaks from 416 to 584 nm was attributed to increase of Cu content in Ag–Cu alloy NPs. In another research, Jiang and coworkers reported a single LSPR peak corresponding to Ag-Cu alloy NPs in the visible region [78]. They further noted that two individual peaks at 407 and 585 nm should be detected if these NPs are pure Ag and Cu, respectively. Therefore, the single peak showed up between these two peaks could be interpreted as Ag–Cu alloy NPs, rather than a mixture of Ag NPs and Cu NPs. Grouchko et al. synthesized Cu-Ag core-shell NPs in aqueous medium. They observed LSPR peak corresponding to Cu NPs at $\sim$ 570 nm [79]. Addition of increasing amounts of silver nitrate resulted in a silver shell formation which was accompanied by the appearance and growth of the 410 nm silver plasmon peak. There are several reports describing composition-tunable plasmonic properties of colloidal Au-Cu alloy NPs. For example, Schaak et al. observed red shift in LSPR peak with increasing Cu content in AuCu alloy NPs obtained by a modified polyol method [124]. In another

study, Sonnichsen and co-workers reported tunable plasmonic properties in colloidal Au-Cu nanorods synthesized using a seed-based growth [63]. In a recent report by Zeng et al. demonstrated modulation of LSPR peaks from visible of near infra-red region in Au-Cu pentacle particles [125]. The appearance of several peaks was attributed to dipoles and higher order multipoles. Liz-Marzán and coworkers reported the tuning of LSPR peaks from visible to infra-red and *vice versa* utilizing spherical and nanorod Au seeds in a shape-templated growth of Au@Cu NPs [126].

1.10 Characterization of NPs

Determination of the nanoparticle structures and the investigation of their chemistry as well as imperfections (e.g. defects) are crucial in order to understand how the material properties relate to their composition and structure. Characterization tools using different probes (e.g. X-ray, neutrons and electrons) can provide information on the structural features in materials such as the three-dimensional arrangement of atoms from sub-Å to sub-micron length scales [127–129]. The advent of modern transmission electron microscopes has offered a unique opportunity to investigate nanomaterials structures using various techniques including high-resolution imaging, diffraction and spectroscopy techniques. The ever-growing development of transmission electron microscopy techniques has enabled scientists to gain a deeper understanding of the structural features of nanomaterials at atomic scale.

1.10.1 TEM Investigations of NPs

Many TEM and HRTEM investigations focus on a microscopic analysis of the structure and the composition of materials at the atomic scale. Approaches to access this information can be put together into two groups. One consists of building especially dedicated equipment such as energy filtered TEM [130], electron energy loss spectroscopy EELS [131] or Z-Contrast Microscopy [132]. The other one makes use of the fact that microscopes produce images for example, HRTEM image. The HRTEM images are electron interferrograms. This is why any quantitative approach to interpret the pattern displayed by a lattice image requires theoretical guidance. The underlying physical process involved in lattice image formation is electron scattering at the crystal potential. Since this potential holds all information about the structure, composition and thickness of the investigated sample it is principally recoverable from any lattice image. However, experimental parameters, such as lens aberrations or the setting of the defocus modifies the pattern of lattice images. Thus, image simulations are required to understand and interpret the contrast of experimentally acquired HRTEM images. There are several methods to compute the interaction of fast electrons with the sample such as Bloch wave and multislice approaches. In this thesis, multislice image simulations are carried out to quantify the lattice images.

1.10.2 Multislice image simulation

High resolution TEM images are not directly interpretable and cannot be used for chemical identification of atoms as these images are formed upon interference of the direct

electron beam with the diffracted beams, the phase part of which is lost upon reaching the image plane. The situation becomes even more complicated as the exit wave function is further been modified by the instrument aberrations. Hence, it is essential to simulate the propagation of the fast electrons inside a specimen which provides insight into the imaging process and helps to interpret the experimental results properly. Careful comparisons between the simulated and the experimental images often reveal the key structural and compositional information about a specimen which cannot be inferred by simple inspection of the experimental results alone. Such examples are found in chapter 8 of the thesis where multislice simulation are performed to explain the experimental observations as well as to retrieve useful information from the experimental data. In the present thesis, the image simulations were performed using Java based EMS software developed by P. Stadelmann [133]. In the chapter 8 of the thesis, multislice simulation has been carried out to simulate cF4 cubic Ag, cF4 Au structure and cP4 phase of Cu3Au intermetallic structure. In all the cases, high resolution images have been simulated under varying thickness and defocus condition along different zone axes through JEMS software. For some of these systems projected potential, exit wave, phase and amplitude part of the exit waves have also been simulated with varying thickness. The single atom potentials for elemental Ag, Au and Cu are determined through Hartree-Fock method by solving the parametric equations as described by Kirkland [134]. The cF4 cubic Ag and Au phases have a lattice parameters 0.4086 nm (PDF card no. 01-073-6976) and 0.4078 nm (PDF card no. 00-004-0784) respectively, with their space group $Fm\bar{3}m$. The cF4 phase has

fourteen 'a' type positions out of which eight positions have coordinates 000 type and remaining six posses $\frac{1}{2}\frac{1}{2}0$ type. In order to simulate the results, pure Ag and Au lattice has been generated through symmetry operation of the point groups using the crystallographic information available in Pearson's handbook [135]. In similar fashion, structures corresponding to the ordered cubic phase (space group: $Pm\bar{3}m$) of Cu_3Au (a $\sim$ 0.375 nm) has also been generated by symmetry operation of the point groups using the available crystallographic information [135]. For all of these structures, high resolution images have been simulated under varying thickness and defocus condition by JEMS software [133]. The simulated thickness-defocus maps generated in all the cases are systematically compared with the experimentally recorded high resolution images.

1.11 Hydrolysis of starch

In this work, a substantial part (chapters 3 and 4) has been devoted to green synthesis. As mentioned in section 1.1, Sella rice has been used as a green source of starch in this part of work. Hereafter, it will be referred to as rice-starch. This has been utilized in syntheses of Ag, Au, Ag-Cu, and Au-Cu NPs. This acted as reducing agents as well as stabilizer for Ag and Au NPs. For Cu, Ag-Cu, and Au-Cu NPs rice- starch was used as stabilizer. It is worth describing hydrolysis of starch to understand aspects of reduction and stabilization for NPs. Rice constitutes about 76 - 78 % starch, 13 - 14 % moisture, and rest 6 - 8 % proteins, fibres, and fats. The rice-starch normally comprises of $\sim$ 20 % amylose and $\sim$ 80 % amylopectin [136]. The amylose consists of lineal chain structure whereas amylopectin possesses branched structure of glucose units. The relative amount of these two units may

vary depending upon rice varieties. During rice-starch preparation, when rice grains are boiled in de-ionized water, the starch grains swell, and both amylose and amylopectin leach out from the rice-granules. At the subjected temperature of boiling ($\sim$ 95 °C), a very small fraction of both amylose and amylopectin breaks down into smaller chains of a few glucose units owing to glycosidic bonds, exposing more aldehyde groups [137–139]. The chain-breaking process continues during sterilization of the solutions (at 110 °C and 69 kPa), exposing a greater number of aldehyde groups, which act as reducing agent for Au ions. As the precursor solutions of Ag and Au are acidic in nature and pouring them into rice-starch solution increases the H^+ ion concentration in reaction mixture. The amylose and amylopectin can decompose into glucose through acid hydrolysis. This process of acid hydrolysis has been presented in Figure 1.8.

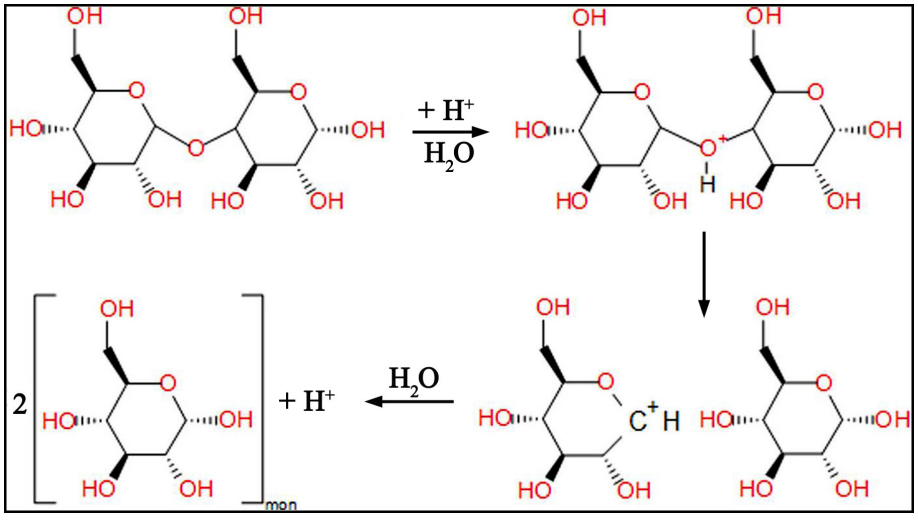

FIGURE 1.8: Hydrolysis of starch in acidic medium [140].

1.12 Objectives of the thesis

The foregoing discussion pertaining to available reports on nanomaterials highlights various facets of synthetic strategies related to elemental and alloy nanoparticles of noble metals. They also demonstrate variation of microstructural and structural features with respect to synthesis parameters. LSPR behaviour of sols and its dependency on morphologies of elemental and alloy nanoparticles have also been discussed in literaure. Influence of nanometric length scale on solid solubilities and structural transformation in Ag-Cu and Au-Cu systems have also been dealt with. Defects and their role in formation of newer phases at nanoscale have not been explored well in literature for Au-Cu system in particular. Investigations on structure and chemistry of nanostructures synthesized through wet chemical method utilizing environmetal friendly stabilizer and their correlation with LSPR behaviour seems to be limited in a sense that is presented here. The thesis proposes to undertake studies to address following issues as a part of objectives. These are:

- Synthesis and characterization of elemental and alloy nanoparticles of Ag, Au, Cu, Ag-Cu and Au-Cu in presence of rice-starch.
- To investigate the influence of pH, concentration of rice-starch, precursors molar ratio, and heat treatments on structures, shape, size, and chemistry of the nanoparticles.
- Effect of other polymeric based processes on shape, size, and chemistry of the nanoparticles of Au and Au-Cu alloy.
- Studies of LSPR behaviour of sols and their stability.

- Investigation of defect mediated morphological and structural transformations in Au-Cu nanoparticles.

- To understand nature of chemistry and structural details of nanoparticles through nano-beam diffraction (NBD), HAADF-STEM-EDS, and HRTEM techniques.

- Contrast interpretation of HRTEM images through simulation.